IEEE Access
Multidisciplinary | Rapid Review | Open Access Journal

Received May 22, 2018, accepted July 2, 2018, date of publication August 3, 2018, date of current version September 7, 2018.

Digital Object Identifier 10.1109/ACCESS.2018.2862887

A Tunable Dual-Band Bandpass-to-Bandstop Filter Using p-i-n Diodes and Varactors

FU-CHANG CHEN, (Member, IEEE), RUN-SHUO LI, AND JI-PENG CHEN
School of Electronic and Information Engineering, South China University of Technology, Guangzhou 510640, China

Corresponding author: Fu-Chang Chen (chenfuchang@scut.edu.cn)

This work was supported in part by the National Natural Science Foundation of China under Grant 61571194, in part by the Science and Technology Planning Project of Guangdong Province under Grant 2014A010103013, in part by the Pearl River Nova Program of Guangzhou under Grant 201610010095, and in part by the Fundamental Research Funds for the Central Universities.

ABSTRACT In this paper, a tunable dual-band bandpass-to-bandstop filter and its analysis are proposed. The bandpass-to-bandstop transformation could be obtained by changing the state of the p-i-n diode. Using two sets of half-wavelength resonators loaded with varactors, the center frequency of each band can be tuned independently by adjusting the varactors. In order to achieve the controlling of the external quality factors (Q_e) for the bandpass mode, the feeding lines are loaded with two varactors and wide tuning range of Q_e can be obtained. In the bandpass mode, the lower passband tuning range is from 1.7 to 2.2 GHz (25.6% tuning range) with return loss better than 10.5 dB, and the tuning range of higher passband is from 2.2 to 2.7 GHz (20.4% tuning range) with return loss better than 12.9 dB. For the bandstop mode, the lower stopband tuning range is from 1.7 to 2.3 GHz (30% tuning range) and the higher stopband tuning range is from 2.3 to 2.9 GHz (23.1% tuning range), while the rejection level is higher than 16.4 dB in the stopband.

INDEX TERMS Bandpss-to-bandstop filter, dual-band, PIN diode, varactor.

I. INTRODUCTION

RF/Microwave tunable filters are required in reconfigurable systems to effectively utilize the frequency spectrum [1]. Tunable filters can also be to replace the filter banks in special systems. Various tunable filters have been designed using different tunable devices, such as ferroelectric capacitor [2], [3], PIN diode [4], micro-electromechanical system (MEMS) device [5]–[8], piezoelectric transducer [9], and varactor diode [10]–[15].

Some research on tunable dual-band filters has been carried out recently [16]–[25]. In [16]–[18] only one passband can be tuned while the other passband is fixed. In [19], a tunable dual-band bandpass filter has been proposed, however, two passbands are dependent and can't be tuned independently. In [20], a high-selectivity dual-band bandpass filter was presented. A novel dual-band filter using dual-mode resonators with independently tunable passband frequencies was proposed in [21]. In [25], a tunable dual-band filter with harmonic suppression was presented.

In the other hand, the bandpass-to-bandstop filters have been developed to receive the desired signal in the dynamic interference environment [26]–[31]. The bandpass mode could be chosen in the low inference environment to receive the desired signal, and the bandstop mode is used to eliminate the high power inference in a high interference environment [26]. In [27], a tunable bandpass-to-bandstop filter has been demonstrated by controlling the coupling coefficient. Tunable bandpass-to-bandstop filters using RF MEMS switches were presented in [28]. Using conventional bandpass and bandstop design theory, a bandpass-to-bandstop filter was presented in [29]. In [30], a tunable bandpass-to-bandstop filter with PIN diodes acting as switch was proposed.

Though tunable dual-band filter and bandpass-to-bandstop filter are widely designed, the design of tunable dual-band bandpass-to-bandstop filter is seldom reported. A bandpass-to-bandstop dual-band filters using RF-MEMS switches with tunable bandwidths was proposed in [31], however, only the bandwidth can be tuned. Following [31], the same method for switching the bandpass and bandstop mode is used in this paper. But unlike using RF MEMS switch in [31], PIN diode is selected to achieve the bandpass-to-bandstop transmission. Using two pairs of half-wavelength resonators loaded with varactors, the dual-band performance can be easily obtained. Furthermore, the center frequency of each band in the bandpass or bandstop mode can be controlled independently.

II. ANALYSIS OF PRESENTED FILTER

In this section, the detailed analysis of the proposed filter is presented. First, an analysis of the tunable filter will be presented in Part A. Then the analysis of the controllable Q_e is illustrated in Part B. Lastly, the structure parameters and the simulated results will be given in Part C.

A. ANALYSIS OF THE PROPOSED FILTER

Following [32], the configuration of presented tunable dual-band bandpass-to-bandstop filter is shown in Fig. 1. It is composed of two pair of diffident half-wavelength resonators loaded with varactors (D_4, D_5, D_6 and D_7). The feeding lines are also loaded with two varactors (D_2 and D_3), which can control the Q_e (external quality factor). The PIN diode (D_1) is placed between the feeding line and the ground acting as a switching device. When V_1 is selected as 0 V, the filter is in the bandstop mode for the PIN diode is in the isolation mode. When $V_1 > 3$ V, the bandpass mode is achieved for the PIN diode is in the thru mode. In Fig. 1, D_2-D_7 are varactors which are controlled by the DC bias voltages named V_2-V_7.

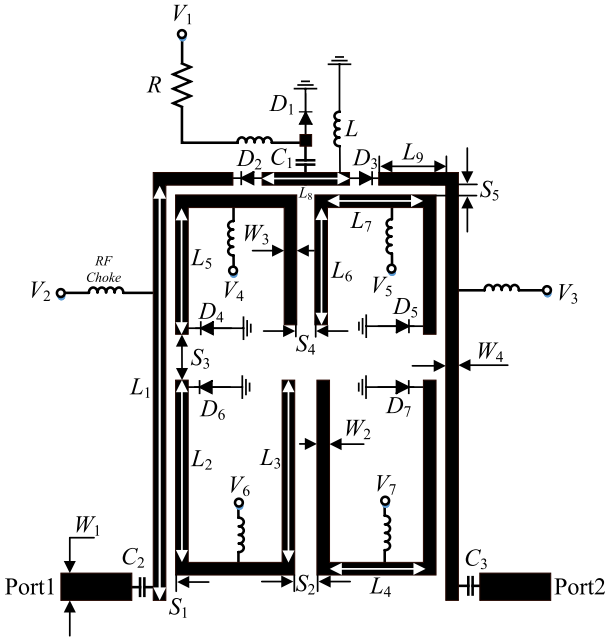

FIGURE 1. Configuration of the proposed tunable dual-band bandpass-to-bandstop filter.

Generally, a smaller Q_e can be obtained with smaller gap between resonators and feeding lines [9]. Therefore, 0.2 mm gap for dual bands is selected to achieve a stronger coupling. Thus, $S_1 = S_5 = 0.2$ mm is selected in this paper.

In Fig. 2, it can be observed that two different coupling paths are applied in the proposed tunable dual-band bandpass-to-bandstop filter. The Path 1 is selected to transmit the lower frequency (1.95 GHz), while the Path 2 is used to transmit the higher frequency (2.45 GHz). At the same time, the distance (S_3) between the two pair of half wavelength resonators is selected as 1.2 mm to reduce the influence between two coupling paths. So the center frequency of

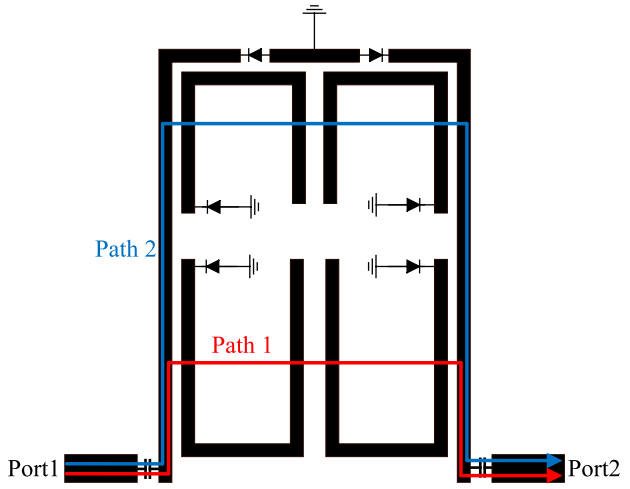

FIGURE 2. Coupling paths of the proposed filter in the bandpass mode.

the passband or stopband can be changed independently by tuning the corresponding DC bias voltage.

In order to analyze the coupling between the half-wavelength resonators, here we take the higher passband as an example, as shown in Fig. 3. The input even/odd admittance is

$$Y_{\text{ine}} = j\omega C_v + Y_1 \frac{Y_{\text{Le}} + jY_1 \tan\theta_1}{Y_1 + jY_{\text{Le}} \tan\theta_1} \quad (1)$$

$$Y_{\text{ino}} = j\omega C_v + Y_1 \frac{Y_{\text{Lo}} + jY_1 \tan\theta_1}{Y_1 + jY_{\text{Lo}} \tan\theta_1} \quad (2)$$

where C_v is the capacitance for D_4 and D_5. And Y_{Le} and Y_{Lo} can be given as

$$Y_{\text{Le}} = jY_{2e} \tan\theta_{2e} \quad (3)$$

$$Y_{\text{Lo}} = jY_{2o} \tan\theta_{2o} \quad (4)$$

The resonate frequency can be calculated from

$$Im(Y_{\text{ine}}) = Im(Y_{\text{ino}}) = 0 \quad (5)$$

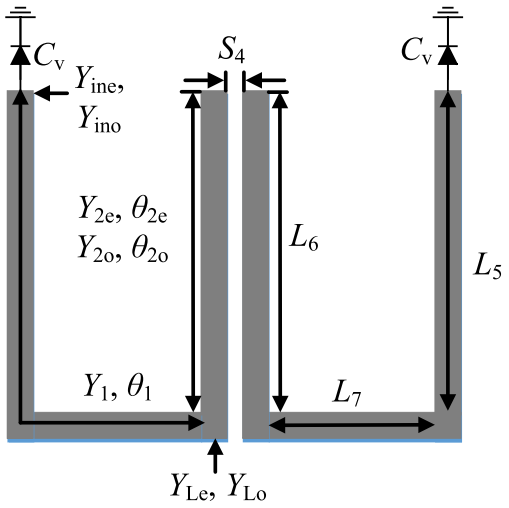

FIGURE 3. Structure of the higher passband resonator.

From (1)-(5), the even/odd mode resonant frequency can be calculated as

$$2\pi f_{0e}C_v = Y_1 \frac{Y_{2e}\tan(\frac{2\pi f_{0e}L_6}{v_p}) + Y_1\tan[\frac{2\pi f_{0e}(L_5+L7)}{v_p}]}{Y_{2e}\tan[\frac{2\pi f_{0e}(L_5+L7)}{v_p}]\tan(\frac{2\pi f_{0e}L_6}{v_p}) - Y_1} \quad (6)$$

$$2\pi f_{0o}C_v = Y_1 \frac{Y_{2o}\tan(\frac{2\pi f_{0o}L_6}{v_p}) + Y_1\tan[\frac{2\pi f_{0o}(L_5+L7)}{v_p}]}{Y_{2o}\tan[\frac{2\pi f_{0o}(L_5+L7)}{v_p}]\tan(\frac{2\pi f_{0o}L_6}{v_p}) - Y_1} \quad (7)$$

Where v_p is the phase velocity, f_{0e} is the even mode resonant frequency and f_{0o} is the odd mode resonant frequency. From (6) and (7), it is shown when Y_1, $Y_{2e/2o}$, $L_5 + L_7$, L_6 and v_p are fixed, the even/odd mode resonant frequency can be tuned by C_v. Additionally, when Y_1 is changed the resonant frequency will be changed accordingly. In order to simplify the design process, Y_1 is fixed and selected as 0.0125 S in this paper. Y_{2e} and Y_{2o} are affected by the coupling coefficient between resonators. So the coupling coefficient will be studied next.

The coupling coefficient k can be express as follow [25]:

$$k = \frac{Im[Y_{12}(\omega_0)]}{\frac{\omega_0}{2}\frac{\partial Im[Y_{11}(\omega_0)]}{\partial\omega}} \quad (8)$$

where

$$Y_{11} = \frac{Y_{ine} + Y_{ino}}{2} \quad (9)$$

$$Y_{12} = \frac{Y_{ine} - Y_{ino}}{2} \quad (10)$$

Form (8), k is determined by the coupling section L_6 and gap (S_4) between the resonators. The presented dual-band tunable bandpass-to-bandstop filter is designed on the substrate with $\varepsilon_r = 2.55$, $\delta = 0.0029$ and $h = 0.8$ mm. The relationship between coupling coefficient and L_6, g_1 at the center frequency of higher tuning range (2.45GHz) are shown in Fig. 4 (a) and (b). From Fig. 4, it can be observed that when the gap between the resonators increases, the coupling coefficient decreases, but the coupling coefficient will increase when L_6 increases. Moreover, S_4 has a major impact on k. Therefore, the required k could be obtained with proper S_4. In this paper, $S_4 = 0.66$ mm and $L_6 = 7.83$ mm are chosen to achieve designed k. Using similar analysis, $S_2 = 1.28$ mm and $L_3 = 14.5$ mm are chosen for the lower passband filter.

B. ANALYSIS OF CONTROLLABLE Q_e

The controllable Q_e can help to acquire good passband performance. In order to control the Q_e, the feeding lines are also with two varactors.

The Q_e for the proposed tunable dual-band bandpass-to-bandstop filter could be extracted from [21]

$$Q_{eh} = \pi f_h \tau_{S_{11h}} \quad (11)$$

$$Q_{el} = \pi f_l \tau_{S_{11l}} \quad (12)$$

where f_h and f_l are the center frequency of the higher passband and lower passband. $f_h = 2.45$ GHz and $f_l = 1.95$ GHz are selected to analyze Q_e. τ_{S11h} and τ_{S11l} are group delays

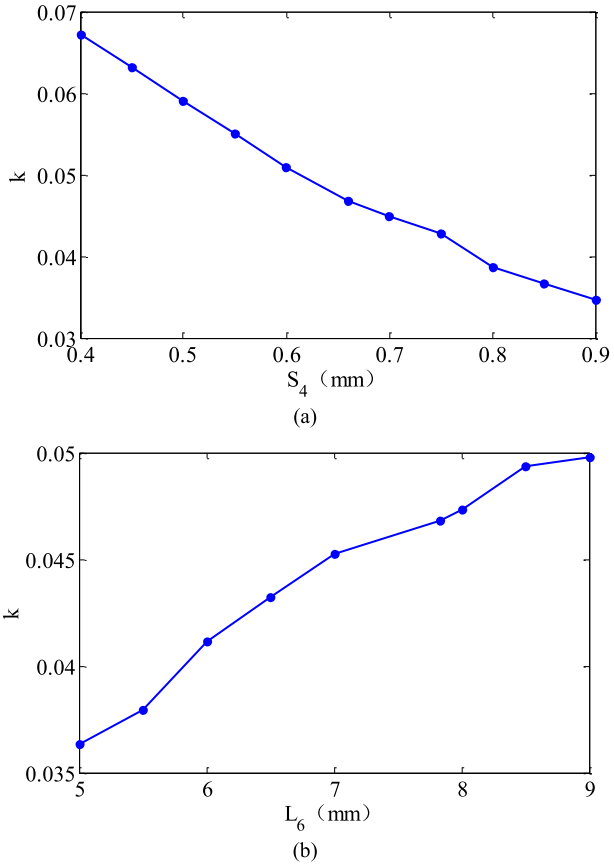

FIGURE 4. Coupling coefficients under different parameters. (a) S_4 ($L_6 = 7.83$ mm). (b) L_6 ($S_4 = 0.66$ mm).

of S_{11} at f_h and f_l, which can be can be extracted by using EM simulation [1]. Fig. 5 shows the structure for studying the controllable Q_e. C_{D2} is the capacitance of the varactor D_2 loaded at the feeding line in Fig. 1. C_{D4} and C_{D6} are the capacitances of the varactors (D_4 and D_6) loaded at the resonators in Fig. 1. C_{D4} and C_{D6} can be tuned to obtain the frequency of f_h and f_l, then C_{D2} is tuned to obtain different Q_e. The parameters are set as follows: $L_1 = 29.3$ mm, $L_8 = 5$ mm, $L_9 = 5.6$ mm. From Fig. 6, when C_{D2} increass, the Q_e

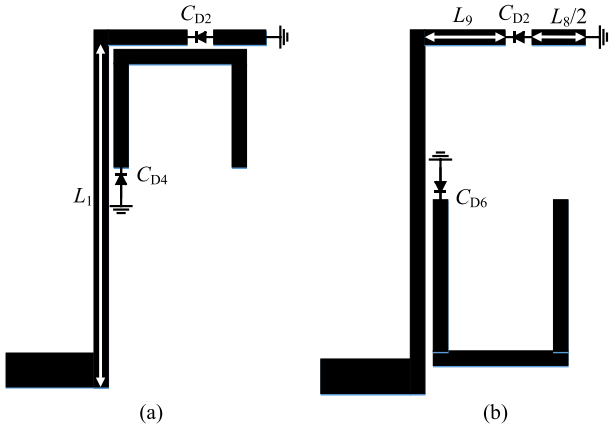

FIGURE 5. The structure to analyze the controllable Q_e. (a) Higher passband resonator. (b) Lower passband resonator.

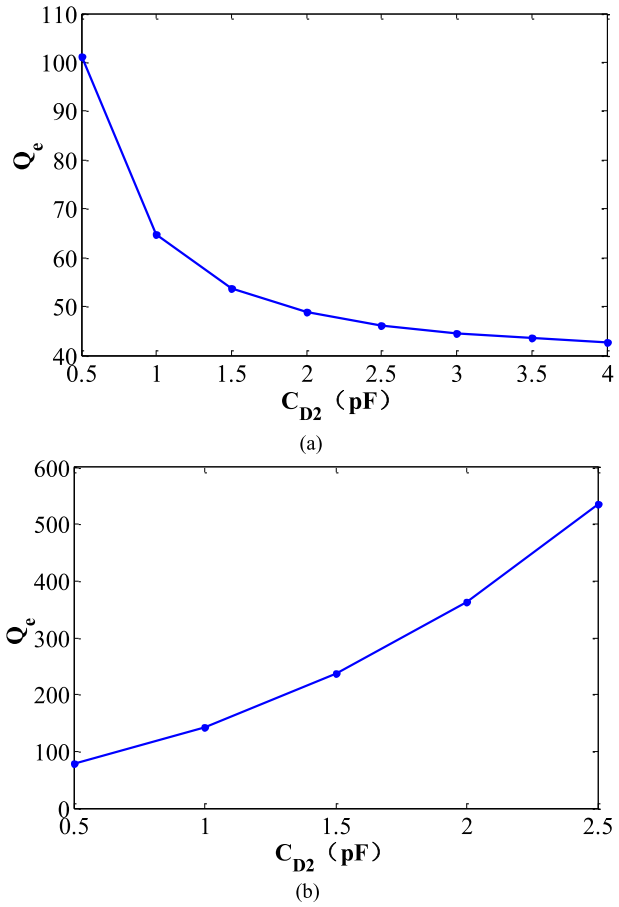

FIGURE 6. Studies of controllable Q_e. (a) Higher passband resonator at $f_h = 2.45$ GHz. (b) Lower passband resonator at $f_l = 1.95$ GHz.

for higher passband decrease, while the Q_e increases for the lower passband. Therefore, the desired Q_e could be obtained by changing the DC bias voltage, V_2 and V_3 in Fig. 1, which are loaded at the varactor D_2 and D_3.

C. SIMULATED RESULTS

From the analysis in Part A and Part B, the physical parameters for the dual-band tunable bandpass-to-bandstop filter can be obtained: $L_1 = 29.3$ mm, $L_2 = 14.5$ mm, $L_3 = 14.5$ imm, $L_4 = 5.26$ mm, $L_5 = 8.8$ mm, $L_6 = 7.83$ mm, $L_7 = 6.57$ mm, $L_8 = 5$ mm, $L_9 = 5.6$ mm, $S_1 = 0.2$ mm,

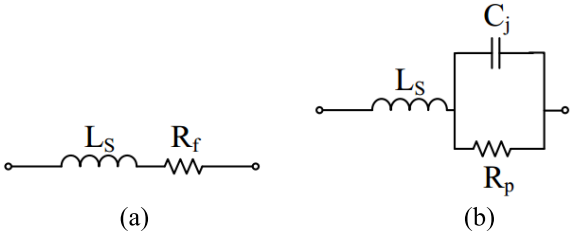

FIGURE 7. Equivalent circuit models for PIN diode BAP64-02. (a) Thru-mode. (b) Isolation.

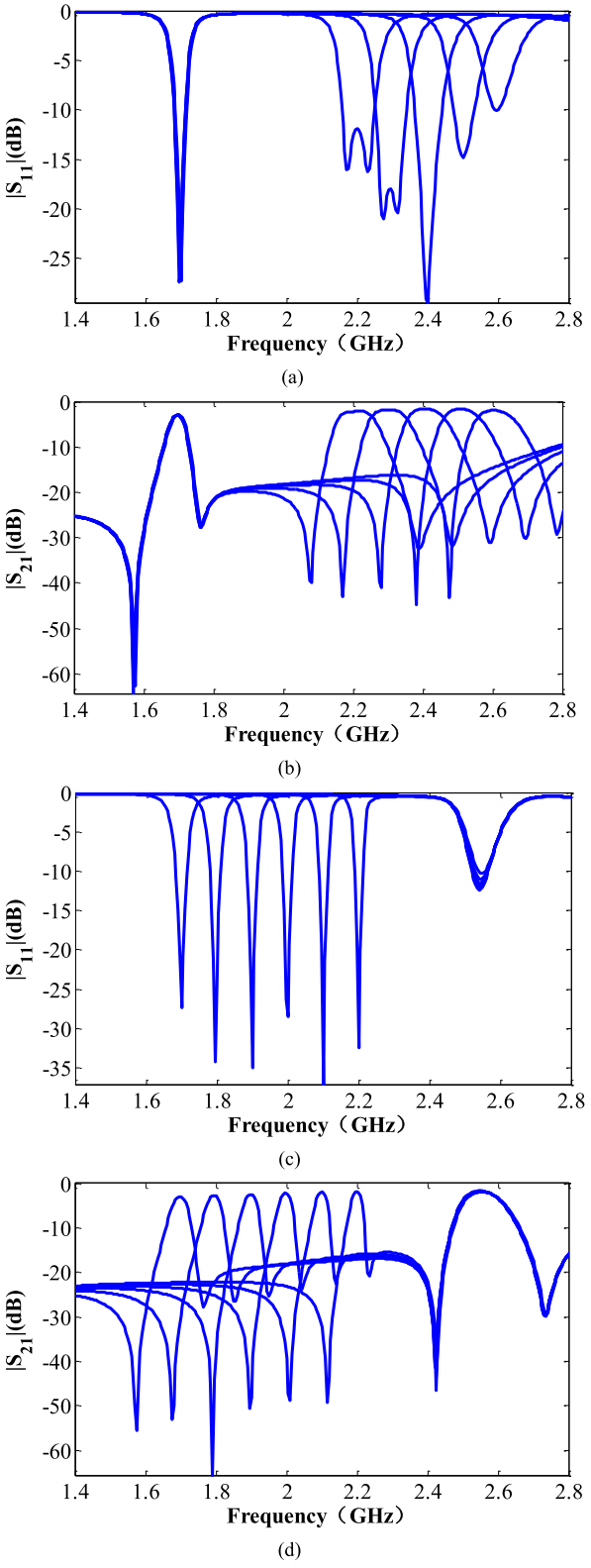

FIGURE 8. Simulated results of the proposed filter in bandpass mode. (a) $|S_{11}|$ with fixed lower passband. (b) $|S_{21}|$ with fixed lower passband. (c) $|S_{11}|$ with fixed higher passband. (d) $|S_{21}|$ with fixed higher passband.

$S_2 = 1.28$ mm, $S_3 = 1.2$ mm, $S_4 = 0.66$ mm, $S_5 = 0.2$ mm, $W_1 = 2.2$ mm, $W_2 = 1$mm, $W_3 = 1$mm, $W_4 = 1$ mm. SMV 1405 varactors ($C_V = 2.67$-0.63 pF, $C_p = 0.29$ pF,

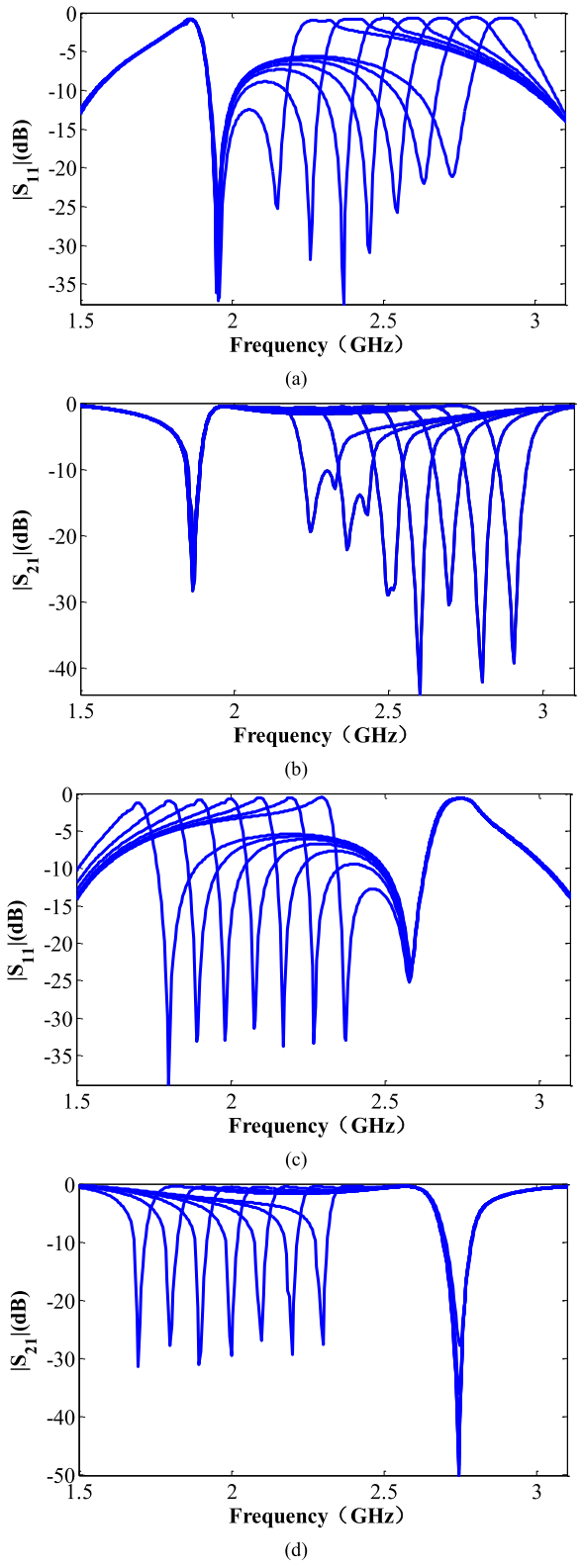

FIGURE 9. Simulated results of the proposed filter in bandstop mode. (a) $|S_{11}|$ with fixed lower passband. (b) $|S_{21}|$ with fixed lower passband. (c) $|S_{11}|$ with fixed higher passband. (d) $|S_{21}|$ with fixed higher passband.

$L_s = 0.7$ nH, $R_s = 0.80\ \Omega$) are used for D_2-D_7. RF choke is achieved with a 270 nH inductor to avoid the RF signal leakage into the DC network. Moreover, an inductor $L = 15$ nH is selected to connect the feeding line with the ground. The PIN diode BAP64-02 is selected to be the switching device. The equivalent circuit model of BAP64-02 is shown in Fig. 7. The parameters of the equivalent circuit for PIN diode are listed as: $R_f = 1\ \Omega$, $L_S = 0.6$ nH, $R_p = 10$ kΩ, $C_j = 0.28$ pF. A resistance $R = 1$ kΩ is selected to be loaded between the DC bias and the feeding line for limiting the current. The chip capacitances C_1-C_3 are used as DC blocking capacitances to avoid the inference. All simulations are performed in ADS. The bandpass mode and bandstop mode simulation results are shown in Fig. 8 and Fig. 9, respectively. It can be observed that each band can be tuned independently.

III. FABRICATION AND MEASUREMENT

A dual-band bandpass-to-bandstop filter is fabricated for verification. Fig. 10 shows the photograph of the presented filter. It can be observed that the total size is 35.2 mm × 36.6 mm, which is 0.333 λ_g by 0.346 λ_g, where λ_g is the guided wavelength on the substrate at the center frequency of the lower passband (1.95 GHz).

An Agilent 5230A network analyzer is selected to perform the measurement. When the PIN diode is in thru mode and V_1 is 0 V, the bandpass mode is achieved, which is shown in Fig. 11. The frequency tuning range of higher passband is from 2.2 GHz to 2.7 GHz (20.4% tuning range) with a fixed lower passband. The return loss is higher than 12.9 dB and the insertion loss is 4.6 dB - 5.6 dB. The tuning range of lower passband is from 1.7 GHz to 2.2 GHz (25.6% tuning range) with a fixed higher passband. The return loss is higher than 10.5 dB and the insertion loss is from 4.6 dB to 5.0 dB. Therefore, the center frequency could be changed from 1.7 GHz to 2.7 GHz continuously in the bandpass mode. The insertion loss is affected by the varactor Q [27] and the loss of the PIN diode and chip capacitances. In the future, the using of the RF MEMS switches can help to achieve improvement in insertion loss [33].

When the DC bias voltage for V_1 is $>3V$, the PIN diode is in isolation state, so the bandstop mode is achieved, the measured results are shown in Fig. 12. The center frequency of higher stopband can be tuned from 2.3 GHz to 2.9 GHz

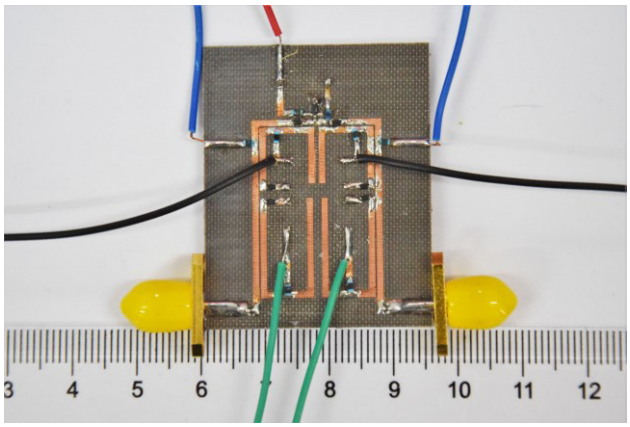

FIGURE 10. Photograph of the fabricated filter.

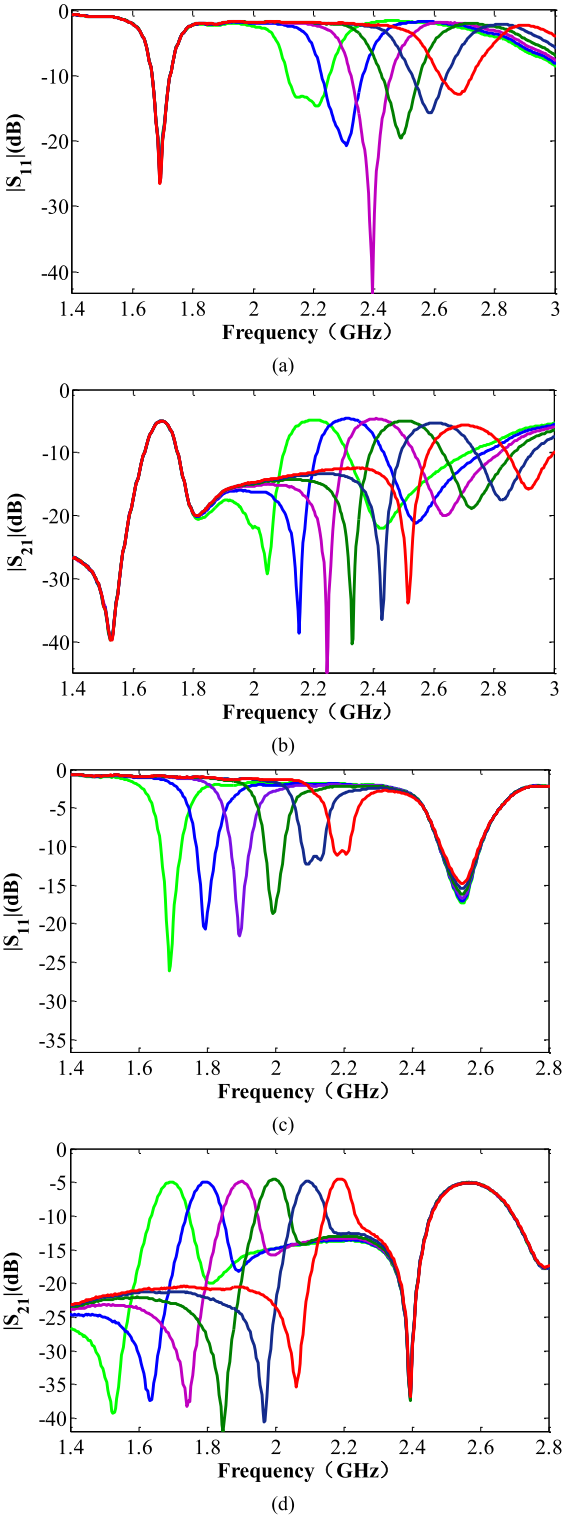

FIGURE 11. Measured results of the proposed filter in bandpass mode. (a) $|S_{11}|$ with fixed lower passband. (b) $|S_{21}|$ with fixed lower passband. (c) $|S_{11}|$ with fixed higher passband. (d) $|S_{21}|$ with fixed higher passband. Bias voltage variation:(a) and (b): $V_2 = V_3 = 30$ V, $V_4 = V_5 = 0 \sim 6$ V, $V_6 = V_7 = 0$ V; (c) and (d): $V_2 = V_3 = 30$ V, $V_4 = V_5 = 3$V, $V_6 = V_7 = 0 \sim 30$ V.

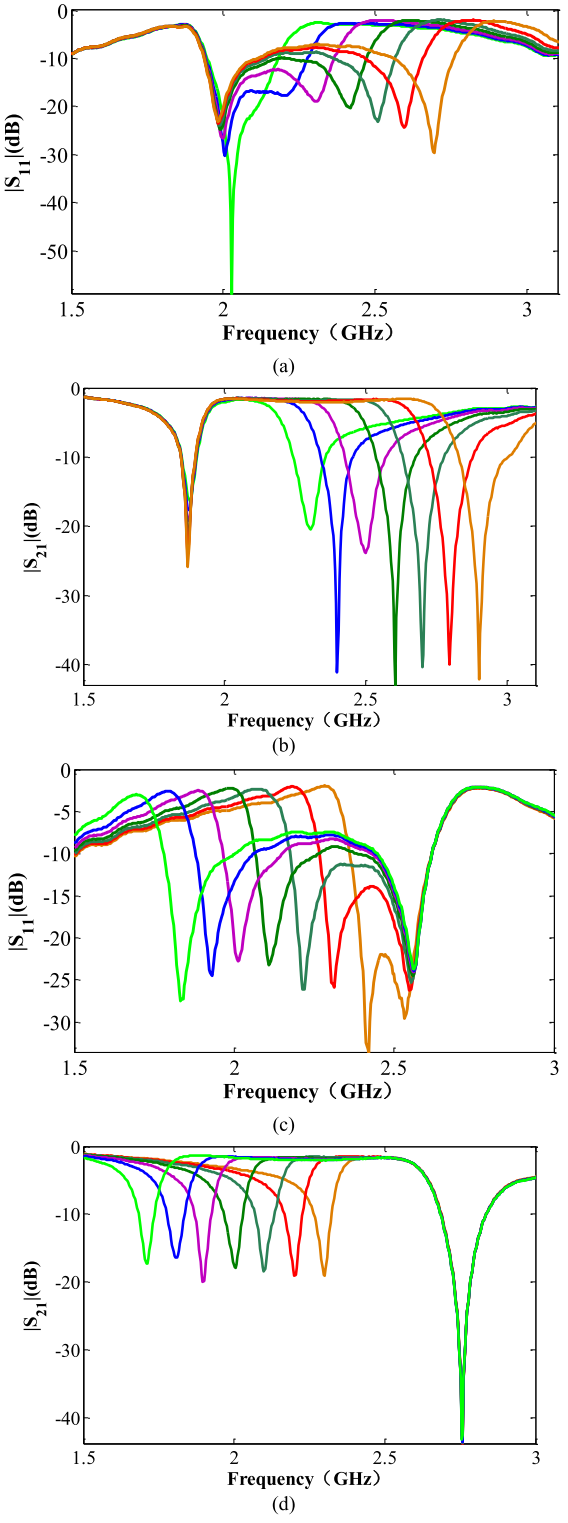

FIGURE 12. Measured results of the proposed filter in bandstop mode. (a) $|S_{11}|$ with fixed lower passband. (b) $|S_{21}|$ with fixed lower passband. (c) $|S_{11}|$ with fixed higher passband. (d) $|S_{21}|$ with fixed higher passband. Bias voltage variation:(a) and (b): $V_2 = V_3 = 0$ V, $V_4 = 0 \sim 18$ V, $V_5 = 0.4 \sim 30$ V, $V_6 = 1.9$ V, $V_7 = 1.6$ V; (c) and (d): $V_2 = V_3 = 0$ V, $V_4 = 7.6$ V, $V_5 = 12$ V, $V_6 = 0.1 \sim 30$ V, $V_7 = 0 \sim 26$ V.

(23.1% tuning range) with a fixed lower stopband, while the rejection level is higher than 20 dB. The lower stopband frequency can be tuned from 1.7 GHz to 2.3 GHz (30% tuning range) with a fixed higher stopband, and the rejection level better than 16.4 dB. Therefore, the stopband can be realized from 1.7 to 2.9 GHz continuously.

TABLE 1. Comparison table.

Filter	Dual-band	Center Frequency tunable	BP-to-BS Switchable	Filter Nature	The Lower channel			The higher channel			Circuit Size ($\lambda_g \times \lambda_g$)
					Frequency tuning (GHz)	IL (dB)	RL (dB)	Frequency tuning (GHz)	IL (dB)	RL (dB)	
[22]	Yes	Yes	No	BPF	1.15-1.72 (39.7%)	4.8-7.6	>12	2.1-2.45 (15.4%)	6.4-11	>10	0.60*0.37
[25]	Yes	Yes	No	BPF	0.88-1.05 (17.6%)	1.4-7.0	>15	1.66-1.87 (11.9%)	3.4-6.7	>20	0.32*0.48
[27]	No	Yes	Yes	BPS	0.78-1.10 (34%)	1.9-4.3	>7.5	-	-	-	-
				BSF	0.77-1.10 (35.3%)	-	>30	-	-	-	
[30]	No	Yes	Yes	BPF	0.81-1.03 (24.7%)	3.1-5.9	>11.5	-	-	-	0.258*0.219
				BSF	0.76-1.23 (47.1%)	-	>40	-	-	-	
[31]	Yes	No	Yes	BPF	0.72	1.4-2.4	>10	1.10	1.8-4.7	>10	-
				BSF	0.70	-	>15	1.09	-	>15	
this work	**Yes**	**Yes**	**Yes**	**BPF**	**1.7-2.2 (25.6%)**	**4.6-5.0**	**>10.5**	**2.2-2.7 (20.4%)**	**4.6-5.6**	**>12.9**	**0.333*0.346**
				BSF	**1.7-2.3 (30%)**	**-**	**>16.4**	**2.3-2.9 (23.1%)**	**-**	**>20**	

IL = Insert Loss; BP = bandpass; BS = bandstop; BPF = bandpass filter; BSF = bandstop filter;
If the filter is bandpass filter or in bandpass mode, RL = return loss. If the filter is bandstop filter or in bandstop mode, RL = rejection level.
λ_g is the guided wavelength on the substrate at the center frequency of the lower passband

Comparisons with some published tunable filters are shown in Table 1. As two sets of resonators are used, this paper can provide a wider tuning range (1 GHz for the bandpass mode and 1.2 GHz for the bandstop mode).

IV. CONCLUSION

A dual-band bandpass-to-bandstop filter with tunable center frequencies is presented in this paper. The PIN diode is used as the switch device here, to change the bandpass-to-bandstop filter transmission. In order to control Q_e, two varactors are loaded at the feeding lines. In the bandpass mode, the frequency can be changed from 1.7 GHz to 2.7 GHz continuously, and in the bandstop mode, the stopband frequency can be tuned from 1.7 GHz to 2.9 GHz continuously. Measured insertion loss in the bandpass mode is limited by the quality factor of the varactor [27] and the loss of the PIN diode. In the future, the using of the RF MEMS component can achieve significant improvement in insertion loss and linearity [33].

REFERENCES

[1] J.-S. Hong, *Microstrip Filters for RF/Microwave Applications*. Hoboken, NJ, USA: Wiley, 2011.

[2] J. Nath *et al.*, "An electronically tunable microstrip bandpass filter using thin-film Barium-Strontium-Titanate (BST) varactors," *IEEE Trans. Microw. Theory Techn.*, vol. 53, no. 9, pp. 2707–2712, Sep. 2005.

[3] H. Jiang, B. Lacroix, K. Choi, Y. Wang, and A. T. H. Papapolymerou, "Ka- and U-band tunable bandpass filters using ferroelectric capacitors," *IEEE Trans. Microw. Theory Techn.*, vol. 59, no. 12, pp. 3068–3075, Dec. 2011.

[4] B. Liu, F. Wei, and X. Shi, "Reconfigurable bandpass filter based on net-type stepped-impedance resonator," *Electron. Lett.*, vol. 46, no. 22, pp. 1506–1507, Feb. 2010.

[5] K. Entesari and G. M. Rebeiz, "A differential 4-bit 6.5-10-GHz RF MEMS tunable filter," *IEEE Trans. Microw. Theory Techn.*, vol. 53, no. 3, pp. 1103–1110, Mar. 2005.

[6] S. Park, M. A. El-Tanani, I. Reines, and G. M. Rebeiz, "Low-loss 4–6 GHz tunable filter with 3-bit high *Q*-orthogonal bias RF-MEMS capacitance network," *IEEE Trans. Microw. Theory Techn.*, vol. 56, no. 10, pp. 2348–2355, Oct. 2008.

[7] F. Huang, S. Fouladi, and R. Mansour, "High-Q tunable dielectric resonator filters using MEMS technology," *IEEE Trans. Microw. Theory Techn.*, vol. 59, no. 12, pp. 3401–3409, Dec. 2011.

[8] K. Entersari and G. M. Rebeiz, "A 12–18 GHz three-pole RF MEMS tunable filter," *IEEE Trans. Microw. Theory Techn.*, vol. 53, no. 8, pp. 2566–2571, Aug. 2005.

[9] L.-H. Hsieh and K. Chang, "Tunable microstrip bandpass filters with two transmission zeros," *IEEE Trans. Microw. Theory Techn.*, vol. 51, no. 2, pp. 520–525, Feb. 2003.

[10] I. C. Hunter and J. D. Rhodes, "Electronically tunable microwave bandpass filters," *IEEE Trans. Microw. Theory Techn.*, vol. MTT-30, no. 9, pp. 1354–1360, Sep. 1982.
[11] S.-J. Park and G. M. Rebeiz, "Low-loss two-pole tunable filters with three different predefined bandwidth characteristics," *IEEE Trans. Microw. Theory Techn.*, vol. 56, no. 5, pp. 1137–1148, May 2008.
[12] W. Tang and J.-S. Hong, "Varactor-tuned dual-mode bandpass filters," *IEEE Trans. Microw. Theory Techn.*, vol. 58, no. 8, pp. 2213–2219, Aug. 2010.
[13] J. Long, C. Li, W. Cui, J. Huangfu, and L. Ran, "A tunable microstrip bandpass filter with two independently adjustable transmission zeros," *IEEE Microw. Wireless Compon. Lett.*, vol. 21, no. 2, pp. 74–76, Feb. 2011.
[14] G. Zhang, Y. H. Xu, and X. D. Wang, "Compact tunable bandpass filter with wide tuning range of centre frequency and bandwidth using short coupled lines," *IEEE Access*, vol. 6, pp. 2962–2969, Dec. 2017.
[15] M. Kheir, T. Kröger, and M. Höft, "A new class of highly-miniaturized reconfigurable UWB filters for multi-band multi-standard transceiver architectures," *IEEE Access*, vol. 5, pp. 1714–1723, Feb. 2017.
[16] D. Girbau, A. Lazaro, A. Perez, E. Martínez, L. Pradell, and R. Villarino, "Tunable dual-band filters based on capacitive-loaded stepped-impedance resonators," in *Proc. 39th Eur. Microw. Conf.*, Sep. 2009, pp. 113–116.
[17] X. Y. Zhang and Q. Xue, "Novel centrally loaded resonators and their applications to bandpass filters," *IEEE Trans. Microw. Theory Techn.*, vol. 56, no. 4, pp. 913–921, Apr. 2008.
[18] G. Chaudhary, H. Choi, Y. Jeong, K. Lim, D. Kim, and J.-C. Kin, "Design of dual-band bandpass filter using DGS with controllable second passband," *IEEE Microw. Wireless Compon. Lett.*, vol. 21, no. 11, pp. 589–591, Nov. 2011.
[19] G. Chaudhary, Y. Jeong, and J. Lim, "Harmonic suppressed dual-band bandpass filters with tunable passbands," *IEEE Trans. Microw. Theory Techn.*, vol. 60, no. 7, pp. 2115–2123, Jul. 2012.
[20] B. You, L. Chen, Y. Liang, and X. Wen, "A high-selectivity tunable dual-band bandpass filter using stub-loaded stepped-impedance resonators," *IEEE Microw. Wireless Compon. Lett.*, vol. 24, no. 11, pp. 736–738, Nov. 2014.
[21] G. Chaudhary, Y. Jeong, and J. Lim, "Dual-band bandpass filter with independently tunable center frequencies and bandwidths," *IEEE Trans. Microw. Theory Techn.*, vol. 61, no. 1, pp. 107–116, Jan. 2013.
[22] T. Yang and G. M. Rebeiz, "Three-pole 1.3–2.4-GHz diplexer and 1.1–2.45-GHz dual-band filter with common resonator topology and flexible tuning capabilities," *IEEE Trans. Microw. Theory Techn.*, vol. 61, no. 10, pp. 3613–3624, Oct. 2013.
[23] Y.-H. Cho and G. M. Rebeiz, "Tunable 4-pole noncontiguous 0.7–2.1-GHz bandpass filters based on dual zero-value couplings," *IEEE Trans. Microw. Theory Techn.*, vol. 63, no. 5, pp. 1579–1586, May 2015.
[24] X. Huang, L. Zhu, Q. Feng, Q. Xiang, and D. Jia, "Tunable bandpass filter with independently controllable dual passbands," *IEEE Trans. Microw. Theory Techn.*, vol. 61, no. 9, pp. 3200–3208, Sep. 2013.
[25] W. Feng, Y. Zhang, and W. Che, "Tunable dual-band filter and diplexer based on folded open loop ring resonators," *IEEE Trans. Circuits Syst. II, Exp. Briefs*, vol. 64, no. 9, pp. 1047–1051, Sep. 2017.
[26] E. J. Naglich, J. Lee, D. Peroulis, and W. J. Chappell, "A tunable bandpass-to-bandstop reconfigurable filter with independent bandwidths and tunable response shape," *IEEE Trans. Microw. Theory Techn.*, vol. 58, no. 12, pp. 3770–3779, Dec. 2010.
[27] Y.-H. Cho and G. M. Rebeiz, "Two- and four-pole tunable 0.7–1.1-GHz bandpass-to-bandstop filters with bandwidth control," *IEEE Trans. Microw. Theory Techn.*, vol. 62, no. 3, pp. 457–463, Mar. 2014.
[28] Y.-H. Cho and G. M. Rebeiz, "0.7–1.0-GHz reconfigurable bandpass-to-bandstop filter with selectable 2- and 4-pole responses," *IEEE Trans. Microw. Theory Techn.*, vol. 62, no. 11, pp. 2626–2632, Nov. 2014.
[29] T. Yang and G. M. Rebeiz, "Bandpass-to-bandstop reconfigurable tunable filters with frequency and bandwidth controls," *IEEE Trans. Microw. Theory Techn.*, vol. 65, no. 7, pp. 2288–2297, Jul. 2017.
[30] R. S. Li and F. C. Chen, "A tunable bandpass-to-bandstop filter with controllable bandwidth and high rejection level," *Microw. Opt. Technol. Lett.*, vol. 59, no. 1, pp. 110–113, Jan. 2017.
[31] N. Kumar and Y. K. Singh, "RF-MEMS-based bandpass-to-bandstop switchable single- and dual-band filters with variable FBW and reconfigurable selectivity," *IEEE Trans. Microw. Theory Techn.*, vol. 65, no. 10, pp. 3824–3837, Oct. 2017.
[32] F. C. Chen, Q. X. Chu, and Z. H. Tu, "Design of compact dual- and tri-band bandpass filters using λ/4 and λ/2 resonators," *Microw. Opt. Techn. Lett.*, vol. 51, no. 3, pp. 638–641, Mar. 2009.
[33] G. M. Rebeiz *et al.*, "Tuning in to RF MEMS," *IEEE Microw. Mag.*, vol. 10, no. 6, pp. 55–72, Oct. 2009.

FU-CHANG CHEN (M'12) was born in Fuzhou, Jiangxi, China, in 1982. He received the Ph.D. degree from the South China University of Technology, Guangzhou, Guangdong, China, in 2010. He is currently an Associate Professor with the School of Electronic and Information Engineering, South China University of Technology. His research interests include the synthesis theory and design of microwave filters and associated RF modules for microwave and millimeter-wave applications.

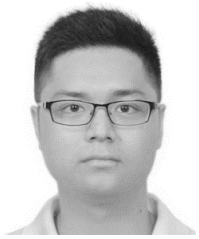

RUN-SHUO LI received the B.S. degree in information engineering from the South China University of Technology, Guangzhou, Guangdong, China, in 2015, where he is currently pursuing the M.E. degree. His research interests include microwave filters and associated RF circuits for microwave and millimeter-wave applications.

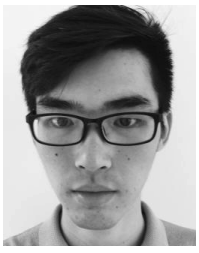

JI-PENG CHEN received the B.S. degree in electronics science and technology from the Guangdong University of Technology, Guangzhou, Guangdong, China, in 2014. He is currently pursuing the M.E. degree with the South China University of Technology. His research interests include microwave components and associated RF circuits for microwave and millimeter-wave applications.